

CODE-VERIFICATION TECHNIQUES FOR AN ARBITRARY-DEPTH ELECTROMAGNETIC SLOT MODEL

Brian A. Freno, Neil R. Matula, Robert A. Pfeiffer, Vinh Q. Dang
Sandia National Laboratories

IEEE International Symposium on Antennas and Propagation
North American Radio Science Meeting
July 13–18, 2025

Sandia National Laboratories is a multimission laboratory managed and operated by National Technology and Engineering Solutions of Sandia, LLC., a wholly owned subsidiary of Honeywell International, Inc., for the U.S. Department of Energy's National Nuclear Security Administration under contract DE-NA-0003525.

Outline

- Introduction
- Governing Equations
- Code-Verification Approaches
- Numerical Examples
- Summary

Outline

- Introduction
 - Electromagnetic Integral Equations
 - Verification and Validation
 - Error Sources
 - This Work
 - Governing Equations
 - Code-Verification Approaches
 - Numerical Examples
 - Summary

Electromagnetic Integral Equations

- Are commonly used to model electromagnetic scattering and radiation
 - Relate surface current to incident electric and/or magnetic field
 - Discretize surface of electromagnetic scatterer with elements
 - Evaluate 4D reaction integrals over 2D test and source elements
 - Contain singular integrands when test and source elements are near

Electromagnetic Aperture and Slot Models

- EM penetration occurs through openings of otherwise closed surfaces
 - Penetration may occur intentionally or unintentionally
 - Slot connects exterior surface of scatterer to interior surface of cavity
 - Model slot as wires carrying magnetic current located at apertures
 - Exterior surface interacts with exterior wire
 - Interior surface interacts with interior wire
 - Exterior and interior wires interact with each other
 - Exterior and interior surfaces do not interact directly

Verification and Validation

Credibility of computational physics codes requires verification and validation

- **Validation** assesses how well models represent physical phenomena
 - Compare computational results with experimental results
 - Assess suitability of models, model error, and bounds of validity
 - **Verification** assesses accuracy of numerical solutions against expectations
 - *Solution verification* estimates numerical error for particular solution
 - *Code verification* verifies correctness of numerical-method implementation

Code Verification

- Code verification most rigorously assesses rate at which error decreases
 - Error requires exact solution – usually unavailable
 - Manufactured solutions are popular alternative
 - Manufacture an arbitrary solution
 - Insert manufactured solution into governing equations to get residual term
 - Add residual term to equations to coerce solution to manufactured solution
 - For integral equations, few instances of code verification exist
 - Analytical differentiation is straightforward – analytical integration is not
 - Numerical integration is necessary, generally incurs an approximation error
 - Therefore, manufactured source term may have its own numerical error

Error Sources in the Electromagnetic Integral Equations

3 sources of numerical error:

- **Domain discretization:** Representation of curved surfaces with planar elements
 - Second-order error for curved surfaces, no error for planar surfaces
 - Error reduced with curved elements
 - **Solution discretization:** Representation of solution or operators
 - Common in solution to differential, integral, and integro-differential equations
 - Finite number of basis functions to approximate solution
 - Finite samples queried to approximate underlying equation operators
 - **Numerical integration:** Quadrature
 - Analytical integration is not always possible
 - For well-behaved integrands,
 - Expect integration error at least same order as solution-discretization error
 - Less rigorously, error should decrease with more quadrature points
 - For (nearly) singular integrands, **monotonic convergence is not assured**

This Work

Isolate solution-discretization error

- Manufacture solution
- Eliminate numerical-integration error by manufacturing Green's function
- Mitigate contamination from discontinuity due to wire–surface interaction

Isolate numerical-integration error

- Manufacture solution
- Cancel solution-discretization error using basis functions

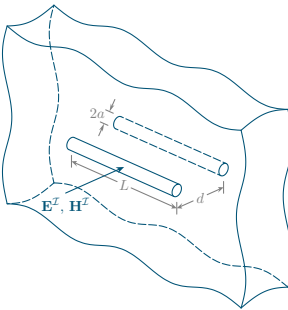
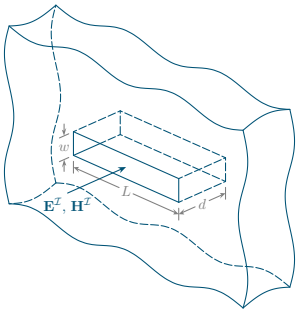
Avoid domain-discretization error

- Consider only planar surfaces
- Previously provided approaches to account for domain-discretization error

Outline

- Introduction
- Governing Equations
 - Overview
 - The Electric-Field Integral Equation
 - The Slot Equation
 - Discretization
- Code-Verification Approaches
- Numerical Examples
- Summary

Arbitrary-Depth Slot Model Overview



- Electromagnetic scatterer of arbitrary depth d encloses a cavity
- Exterior is connected to interior by rectangularly prismatic slot with $L \gg w$ (left)
- Slot is replaced with two thin wires at apertures that carry magnetic current (right)
- Exterior and interior surfaces interact with wires, not each other
- Wires interact with each other through waveguide model
- EFIE solved on each surface, slot equation solved for wires

The Electric-Field Integral Equation

In time-harmonic form, \mathbf{E}^S computed from \mathbf{J} and \mathbf{M}

Scattered electric field $\mathbf{E}^S(\mathbf{x}) = -\left(j\omega \mathbf{A}(\mathbf{x}) + \nabla \Phi(\mathbf{x}) + \frac{1}{\epsilon} \nabla \times \mathbf{F}(\mathbf{x})\right)$

Magnetic vector potential $\mathbf{A}(\mathbf{x}) = \mu \int_{S'} \mathbf{J}(\mathbf{x}') G(\mathbf{x}, \mathbf{x}') dS'$

Electric scalar potential $\Phi(\mathbf{x}) = \frac{j}{\epsilon\omega} \int_{S'} \nabla' \cdot \mathbf{J}(\mathbf{x}') G(\mathbf{x}, \mathbf{x}') dS'$

Electric vector potential $\mathbf{F}(\mathbf{x}) = \epsilon \int_{S'} \mathbf{M}(\mathbf{x}') G(\mathbf{x}, \mathbf{x}') dS'$

Green's function $G(\mathbf{x}, \mathbf{x}') = \frac{e^{-jkR}}{4\pi R}, \quad R = |\mathbf{x} - \mathbf{x}'|$

Singularity when $R \rightarrow 0$

\mathbf{J} and \mathbf{M} are electric and magnetic surface current densities

$S' = S$ is surface of scatterer

μ and ϵ are permeability and permittivity of surrounding medium

$k = \omega\sqrt{\mu\epsilon}$ is wavenumber

The Electric-Field Integral Equation (continued)

Compute \mathbf{J} and \mathbf{M} from incident electric field \mathbf{E}^I $(\mathbf{n} \times (\mathbf{E}^S + \mathbf{E}^I)) = Z_s \mathbf{n} \times \mathbf{J})$

Discretize surface with triangles, approximate \mathbf{J} with RWG basis functions:

$$\mathbf{J}_h(\mathbf{x}) = \sum_{j=1}^{n_b} J_j \boldsymbol{\Lambda}_j(\mathbf{x})$$

Project EFIE onto linear, vector-valued RWG basis functions

Express \mathbf{M} in terms of filament magnetic current \mathbf{I}_m

Discretize wire with bars, approximate \mathbf{I}_m with 1D basis functions:

$$\mathbf{I}_h(s) = \sum_{j=1}^{n_b^m} I_j \boldsymbol{\Lambda}_j^m(s)$$

The Slot Equation

The magnetic current along the slot is modeled using a waveguide model:

$$\mathbf{s} \cdot (\mathbf{J}^\pm \times \mathbf{n}^\pm) + \frac{j\omega\epsilon}{2wL(k^2 - \beta_x^2)} \sum_{p=1}^{\infty} \beta_{y_p} \int_0^L \sin\left(\frac{p\pi s}{L}\right) \sin\left(\frac{p\pi s'}{L}\right) \times$$

$$(\pm [I_m^-(s') - I_m^+(s')] \tan(\beta_{y_p} d/2) + [I_m^+(s') + I_m^-(s')] \cot(\beta_{y_p} d/2)) ds' = 0$$

$$I_m(0) = I_m(L) = 0$$

\mathbf{s} is the direction of the wire ($\mathbf{I}_m = I_m(s)\mathbf{s}$)

Superscripts – and + denote exterior and interior

Effective wire radius a obtained from conformal mapping using w and d

β_α is the propagation constant in the α direction

Project slot equation onto 1D basis functions

Discretized Problem

Find $\mathbf{J}_h \in \mathbb{V}_h$ and $\mathbf{I}_h \in \mathbb{V}_h^m$, such that

$$a_{\mathcal{E},\mathcal{E}}(\mathbf{J}_h, \boldsymbol{\Lambda}_i) + a_{\mathcal{E},\mathcal{M}}(\mathbf{I}_h, \boldsymbol{\Lambda}_i) = b_{\mathcal{E}}(\mathbf{E}^{\mathcal{T}}, \boldsymbol{\Lambda}_i) \quad \text{for } i = 1, \dots, n_b \quad (\text{EFIE})$$

$$a_{\mathcal{M},\mathcal{E}}(\mathbf{J}_h, \boldsymbol{\Lambda}_i^m) + a_{\mathcal{M},\mathcal{M}}(\mathbf{I}_h, \boldsymbol{\Lambda}_i^m) = 0 \quad \text{for } i = 1, \dots, n_b^m \quad (\text{Slot})$$

Evaluate EFIE on exterior and interior surfaces: $n_b^- + n_b^+$ unknowns for \mathbf{J}_h

Evaluate slot equation on exterior and interior wires: $n_b^{m-} + n_b^{m+}$ unknowns for \mathbf{I}_h

Matrix–Vector Form

In matrix–vector form, solve for \mathcal{J}^h :

$$\mathbf{Z}\mathcal{J}^h = \mathbf{V}$$

$$\mathbf{Z} = \begin{bmatrix} \mathbf{A}^- & \mathbf{0} & \mathbf{B}^- & \mathbf{0} \\ \mathbf{0} & \mathbf{A}^+ & \mathbf{0} & \mathbf{B}^+ \\ \mathbf{C}^- & \mathbf{0} & \mathbf{D}_\sim^- & \mathbf{D}_\not\sim^- \\ \mathbf{0} & \mathbf{C}^+ & \mathbf{D}_\not\sim^+ & \mathbf{D}_\sim^+ \end{bmatrix}, \quad \mathcal{J}^h = \begin{Bmatrix} \mathbf{J}^{h-} \\ \mathbf{J}^{h+} \\ \mathbf{I}^{h-} \\ \mathbf{I}^{h+} \end{Bmatrix}, \quad \mathbf{V} = \begin{Bmatrix} \mathbf{V}^{\mathcal{E}-} \\ \mathbf{V}^{\mathcal{E}+} \\ \mathbf{0} \\ \mathbf{0} \end{Bmatrix},$$

Impedance matrix Current vector Excitation vector

where

$$A_{i,j} = a_{\mathcal{E},\mathcal{E}}(\Lambda_j, \Lambda_i), \quad B_{i,j} = a_{\mathcal{E},\mathcal{M}}(\Lambda_j^m, \Lambda_i), \quad C_{i,j} = a_{\mathcal{M},\mathcal{E}}(\Lambda_j, \Lambda_i^m), \quad D_{i,j} = a_{\mathcal{M},\mathcal{M}}(\Lambda_j^m, \Lambda_i^m),$$

$$J_j^h = J_j, \quad I_j^h = I_j, \quad V_j^{\mathcal{E}} = b_{\mathcal{E}}(\mathbf{E}^{\mathcal{I}}, \Lambda_i)$$

More compactly:

$$\mathbf{Z} = \begin{bmatrix} \mathbf{A} & \mathbf{B} \\ \mathbf{C} & \mathbf{D} \end{bmatrix}, \quad \mathcal{J}^h = \begin{Bmatrix} \mathbf{J}^h \\ \mathbf{I}^h \end{Bmatrix}, \quad \mathbf{V} = \begin{Bmatrix} \mathbf{V}^{\mathcal{E}} \\ \mathbf{0} \end{Bmatrix}$$

Outline

- Introduction
- Governing Equations
- Code-Verification Approaches
 - Manufactured Solutions
 - Solution-Discretization Error
 - Numerical-Integration Error
 - Manufactured Green's Function
- Numerical Examples
- Summary

Manufactured Solutions for the EFIE

Continuous: $r_{\mathcal{E}_i}(\mathbf{J}, \mathbf{I}_m) = a_{\mathcal{E}, \mathcal{E}}(\mathbf{J}, \boldsymbol{\Lambda}_i) + a_{\mathcal{E}, \mathcal{M}}(\mathbf{I}_m, \boldsymbol{\Lambda}_i) - b_{\mathcal{E}}(\mathbf{E}^{\mathcal{I}}, \boldsymbol{\Lambda}_i) = 0$

Discretized: $r_{\mathcal{E}_i}(\mathbf{J}_h, \mathbf{I}_h) = a_{\mathcal{E}, \mathcal{E}}(\mathbf{J}_h, \boldsymbol{\Lambda}_i) + a_{\mathcal{E}, \mathcal{M}}(\mathbf{I}_h, \boldsymbol{\Lambda}_i) - b_{\mathcal{E}}(\mathbf{E}^{\mathcal{I}}, \boldsymbol{\Lambda}_i) = 0$

Method of manufactured solutions modifies discretized equations:

$$\mathbf{r}_{\mathcal{E}}(\mathbf{J}_h, \mathbf{I}_h) = \mathbf{r}_{\mathcal{E}}(\mathbf{J}_{MS}, \mathbf{I}_{MS})$$

\mathbf{J}_{MS} and \mathbf{I}_{MS} are manufactured solutions, $\mathbf{r}_{\mathcal{E}}(\mathbf{J}_{MS}, \mathbf{I}_{MS})$ is computed exactly

New Discretized: $a_{\mathcal{E}, \mathcal{E}}(\mathbf{J}_h, \boldsymbol{\Lambda}_i) + a_{\mathcal{E}, \mathcal{M}}(\mathbf{I}_h, \boldsymbol{\Lambda}_i) = \underbrace{a_{\mathcal{E}, \mathcal{E}}(\mathbf{J}_{MS}, \boldsymbol{\Lambda}_i) + a_{\mathcal{E}, \mathcal{M}}(\mathbf{I}_{MS}, \boldsymbol{\Lambda}_i)}_{= b_{\mathcal{E}}(\mathbf{E}^{\mathcal{I}}, \boldsymbol{\Lambda}_i)}: \text{implement via } \mathbf{E}^{\mathcal{I}}$

$$\begin{aligned} \mathbf{E}^{\mathcal{I}}(\mathbf{x}) &= \frac{j}{\epsilon\omega} \int_{S'} [k^2 \mathbf{J}_{MS}(\mathbf{x}') \mathbf{G}(\mathbf{x}, \mathbf{x}') + \nabla' \cdot \mathbf{J}_{MS}(\mathbf{x}') \nabla \mathbf{G}(\mathbf{x}, \mathbf{x}')] dS' + Z_s \mathbf{J}_{MS}(\mathbf{x}) \\ &\quad - \frac{1}{4} (\mathbf{n}(\mathbf{x}) \times \mathbf{I}_{MS}(\mathbf{x})) \delta_{slot}(\mathbf{x}) + \frac{1}{4\pi} \int_0^L \mathbf{I}_{MS}(s') \times \int_0^{2\pi} \nabla' \mathbf{G}(\mathbf{x}, \mathbf{x}') d\phi' ds' \end{aligned}$$

MMS incorporated through $\mathbf{E}^{\mathcal{I}}$ – no additional source term required

Manufactured Solutions for the Slot Equation

Continuous: $r_{\mathcal{M}_i}(\mathbf{J}_m, \mathbf{I}_m) = a_{\mathcal{M}, \mathcal{E}}(\mathbf{J}_m, \Lambda_i^m) + a_{\mathcal{M}, \mathcal{M}}(\mathbf{I}_m, \Lambda_i^m) = 0$

Discretized: $r_{\mathcal{M}_i}(\mathbf{J}_h, \mathbf{I}_h) = a_{\mathcal{M}, \mathcal{E}}(\mathbf{J}_h, \Lambda_i^m) + a_{\mathcal{M}, \mathcal{M}}(\mathbf{I}_h, \Lambda_i^m) = 0$

Method of manufactured solutions modifies discretized equations:

$$\mathbf{r}_{\mathcal{M}}(\mathbf{J}_h, \mathbf{I}_h) = \mathbf{r}_{\mathcal{M}}(\mathbf{J}_{MS}, \mathbf{I}_{MS})$$

New Discretized:

$$a_{\mathcal{M}, \mathcal{E}}(\mathbf{J}_h, \Lambda_i^m) + a_{\mathcal{M}, \mathcal{M}}(\mathbf{I}_h, \Lambda_i^m) = \underbrace{a_{\mathcal{M}, \mathcal{E}}(\mathbf{J}_{MS}, \Lambda_i^m) + a_{\mathcal{M}, \mathcal{M}}(\mathbf{I}_{MS}, \Lambda_i^m)}_{= 0: \text{ no source term needed}}$$

Given \mathbf{J}_{MS} , solve for $\mathbf{I}_m(s) = I_m(s)\mathbf{s}$ to avoid source term

$$J_s(s) = \sum_{q=1}^{\infty} J_{sq} \sin\left(\frac{q\pi s}{L}\right), \quad J_{sq} = \frac{2}{L} \int_0^L J_s(s) \sin\left(\frac{q\pi s}{L}\right) ds,$$

$$I_m(s) = \sum_{q=1}^{\infty} I_{mq} \sin\left(\frac{q\pi s}{L}\right), \quad I_{mq}^{\pm} = \frac{jw(k^2 - \beta_x^2)}{\beta_{yq}\omega\epsilon} ([J_{sq}^+ + J_{sq}^-] \tan(\beta_{yq}d/2) \mp [J_{sq}^+ - J_{sq}^-] \cot(\beta_{yq}d/2))$$

Solution-Discretization Error

- Error due to basis-function approximations of solutions:

$$\mathbf{J}_h(\mathbf{x}) = \sum_{j=1}^{n_b} J_j \boldsymbol{\Lambda}_j(\mathbf{x}), \quad \mathbf{I}_h(s) = \sum_{j=1}^{n_b^m} I_j \boldsymbol{\Lambda}_j^m(s)$$

- Measured with discretization errors: $\mathbf{e}_{\mathbf{J}} = \mathbf{J}^h - \mathbf{J}_n, \quad \mathbf{e}_{\mathbf{I}} = \mathbf{I}^h - \mathbf{I}_s$

$$\|\mathbf{e}_{\mathbf{J}}\| \leq C_{\mathbf{J}} h^{p_{\mathbf{J}}}, \quad \|\mathbf{e}_{\mathbf{I}}\| \leq C_{\mathbf{I}} h^{p_{\mathbf{I}}}$$

J_{n_j} : component of \mathbf{J}_{MS} flowing from T_j^+ to T_j^-

I_{s_j} : component of \mathbf{I}_{MS} flowing along \mathbf{s} at s_j

C : function of solution derivatives

h : measure of mesh size

p : order of accuracy

- Compute p from $\|\mathbf{e}\|$ across multiple meshes (expect $p = 2$ for these bases)
- Avoid numerical-integration error if integrating exactly

Solution-Discretization Error: Discontinuity

- δ_{slot} introduces discontinuity due to wire interaction with surface
- Discontinuity impacts $\mathbf{E}^{\mathcal{I}}$ for MMS
- Discontinuity will contaminate convergence studies: $\mathcal{O}(h^2) \rightarrow \mathcal{O}(h)$
- Discontinuity denoted by \mathbf{B}_1 in $\mathbf{Z} = \begin{bmatrix} \mathbf{A} & (\mathbf{B}_1 + \mathbf{B}_2) \\ \mathbf{C} & \mathbf{D} \end{bmatrix}$
- Since $\mathbf{B}_1 = -\frac{1}{4}\mathbf{C}^T$, use \mathbf{C} to cancel contribution from \mathbf{B}_1 and modify $\mathbf{E}^{\mathcal{I}}$:

$$\mathbf{Z} = \begin{bmatrix} \mathbf{A} & (\cancel{\mathbf{B}_1} + \mathbf{B}_2) \\ \mathbf{C} & \mathbf{D} \end{bmatrix},$$

$$\mathbf{E}^{\mathcal{I}} = \frac{j}{\epsilon\omega} \int_{S'} [k^2 \mathbf{J}_{\text{MS}} G + \nabla' \cdot \mathbf{J}_{\text{MS}} \nabla G] dS' - \cancel{\frac{1}{4}(\mathbf{n} \times \mathbf{I}_{\text{MS}}) \delta_{\text{slot}}} + \frac{1}{4\pi} \int_0^L \mathbf{I}_{\text{MS}} \times \int_0^{2\pi} \nabla' G d\phi' ds' + Z_s \mathbf{J}_{\text{MS}}$$

- Correctness of \mathbf{B}_1 is assessed by successful removal using \mathbf{C}
- Correctness of \mathbf{C} is assessed through the mesh-convergence study

Numerical-Integration Error

- Error due to quadrature integral evaluation $(\cdot)^q$ on both sides of equations
- Measure numerical-integration error:

$$e_a = \mathcal{J}^H(\mathbf{Z}^q - \mathbf{Z})\mathcal{J}, \quad e_b = \mathcal{J}^H(\mathbf{V}^q - \mathbf{V}),$$

where $\mathcal{J} = \begin{Bmatrix} \mathbf{J}_n \\ \mathbf{I}_s \end{Bmatrix}$

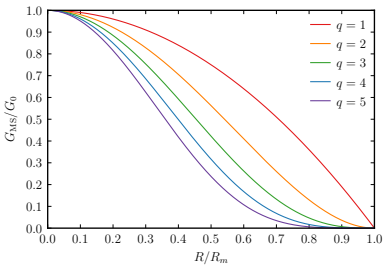
- Solution-discretization error is canceled
- $|e_a| \leq C_a h^{p_a}$ and $|e_b| \leq C_b h^{p_b}$
 - C : function of integrand derivatives
 - p : order of accuracy of quadrature rules
- With multiple meshes, compute p from $|e|$

Manufactured Green's Function

Integrals with G cannot be computed analytically or, when $R \rightarrow 0$, accurately

Inaccurately computing integrals on either side contaminates convergence studies

Manufacture Green's function: $G_{\text{MS}}(R) = G_0 \left(1 - \frac{R^2}{R_m^2}\right)^q$, $R_m = \max_{\mathbf{x}, \mathbf{x}' \in S} R$ and $q \in \mathbb{N}$



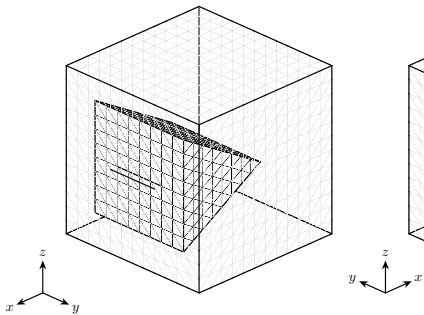
Reasoning:

- 1) Even powers of R permit integrals to be computed analytically
- 2) G_{MS} increases when R decreases, as with actual G

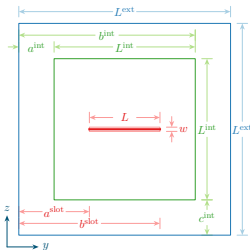
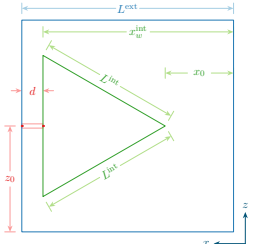
Outline

- Introduction
- Governing Equations
- Code-Verification Approaches
- Numerical Examples
 - Domain and Parameters
 - Manufactured Surface Current
 - Magnetic Current
 - Solution-Discretization Error
 - Numerical-Integration Error
- Summary

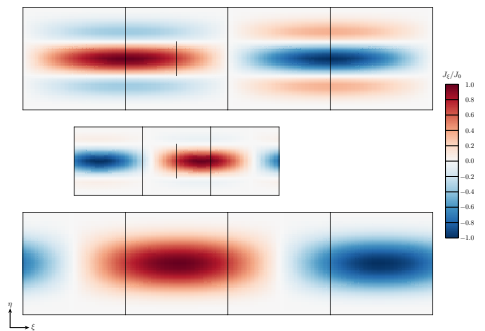
Cubic Scatterer with a Triangularly Prismatic Cavity



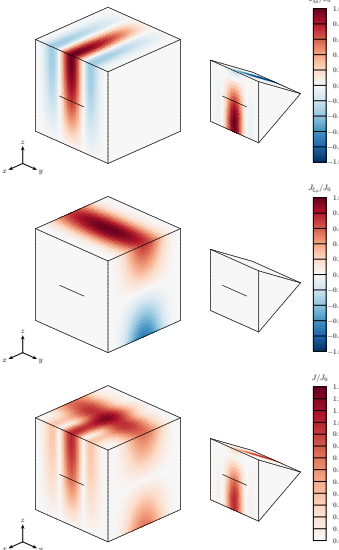
- $L^{\text{ext}} = 1 \text{ m}$, $L^{\text{int}} = 2L^{\text{ext}}/3$, $L = L^{\text{ext}}/3$, $w = L^{\text{ext}}/50$
- $a^{\text{int}} = L^{\text{ext}}/6$, $c^{\text{int}} = L^{\text{ext}}/6$, $z_0 = L^{\text{ext}}/2$
- $\mu = \mu_0$, $\epsilon = \epsilon_0$, $k = 2\pi \text{ m}^{-1}$, $\sigma_{\text{scatterer}} \gg \sigma_{\text{slot}} > \sigma_0 = 0$
- 3 depths: $d_1 = L^{\text{ext}}/5$, $d_2 = L^{\text{ext}}/10$, $d_3 = L^{\text{ext}}/20$
- 2 Green's functions: G_1, G_2



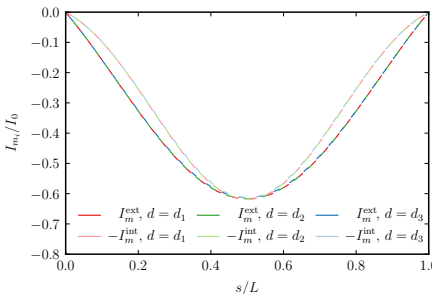
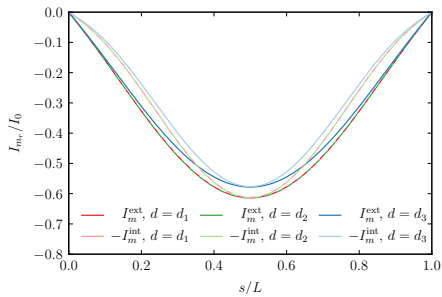
Manufactured Surface Current



- Manufacture solutions for 2D strips of class C^2
- Wrap strips around lateral surfaces of prisms
- Solutions are product of ξ and η dependencies
 - ξ dependency: sine function with single period
 - η dependency: linear combination of odd-harmonic sine functions
- Current flows along ξ ; at $s = \{0, L\}$, $J_\xi = 0$



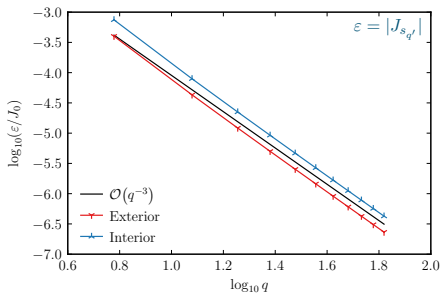
Magnetic Current



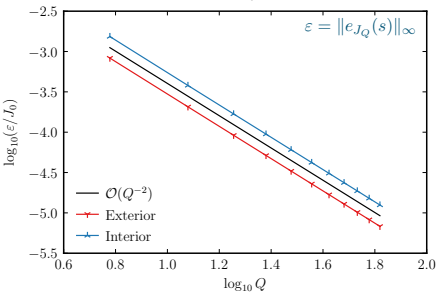
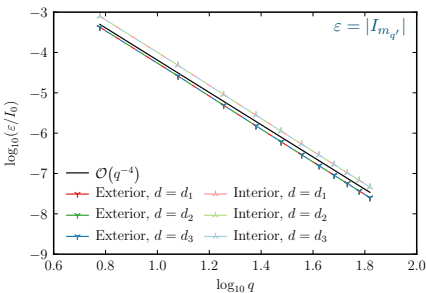
- For a given \mathbf{J}_{MS} , $\mathbf{I}_m(s) = I_m(s)\mathbf{s}$ is an infinite series that needs to be truncated

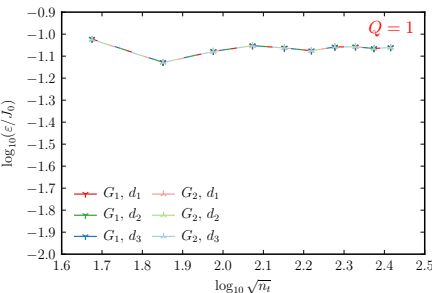
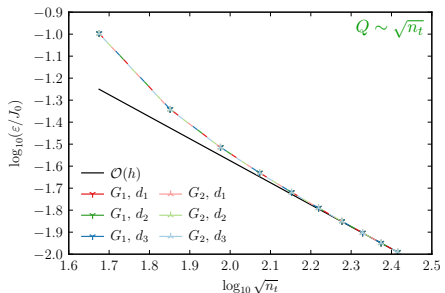
$$I_{m_Q}(s) = \sum_{q=1}^Q I_{m_{q'}} \sin\left(\frac{q'\pi s}{L}\right), \quad q' = 2q - 1$$

Sine Series Convergence



- J_s sine coefficients are $\mathcal{O}(q^{-3})$
- I_m sine coefficients are $\mathcal{O}(q^{-4})$
- $\|e_{J_Q}(s)\|_\infty = \max_{s \in [0, L]} |J_{s_Q}(s) - J_s(s)|$ is $\mathcal{O}(Q^{-2})$
- $\|e_{I_Q}(s)\|_\infty = \max_{s \in [0, L]} |I_{m_Q}(s) - I_m(s)|$ is $\mathcal{O}(Q^{-3})$
- Set $Q \sim \sqrt{n_t}$ to reduce truncation error faster
 - Basis-function error is $\mathcal{O}(h^2)$
 - I_m truncation error is $\mathcal{O}(h^3)$

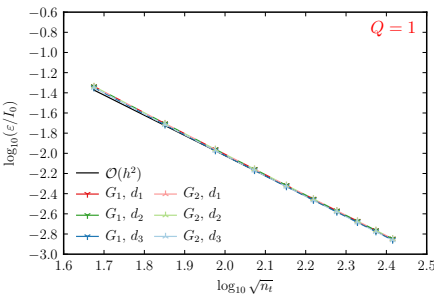
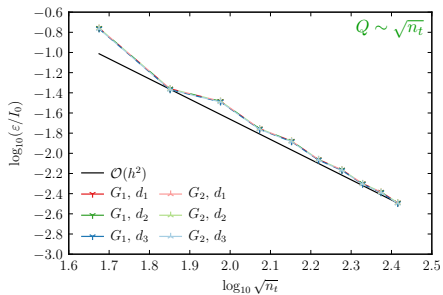


Solution-Discretization Error: $\varepsilon = \|\mathbf{e}_J\|_\infty$ (with discontinuity)

- Discontinuity present:

$$\begin{bmatrix} \mathbf{A} & \mathbf{B} \\ \mathbf{C} & \mathbf{D} \end{bmatrix} \begin{Bmatrix} \mathbf{J}^h \\ \mathbf{I}^h \end{Bmatrix} = \begin{Bmatrix} \mathbf{V}^\varepsilon \\ \mathbf{0} \end{Bmatrix}$$

- Convergence rates for $Q = 1$ and $Q \sim \sqrt{n_t}$ are $\mathcal{O}(1)$ and $\mathcal{O}(h)$

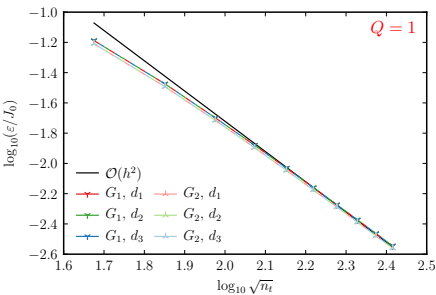
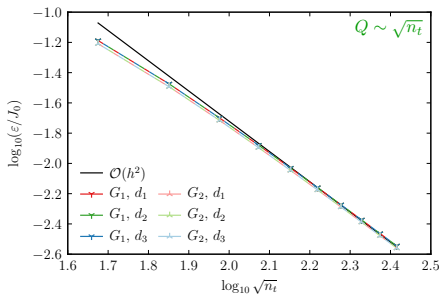
Solution-Discretization Error: $\varepsilon = \|\mathbf{e}_I\|_\infty$ (with discontinuity)

- Discontinuity present:

$$\begin{bmatrix} \mathbf{A} & \mathbf{B} \\ \mathbf{C} & \mathbf{D} \end{bmatrix} \begin{Bmatrix} \mathbf{J}^h \\ \mathbf{I}^h \end{Bmatrix} = \begin{Bmatrix} \mathbf{V}^\varepsilon \\ \mathbf{0} \end{Bmatrix}$$

- Convergence rates for $Q = 1$ and $Q \sim \sqrt{n_t}$ are $\mathcal{O}(h^2)$

Solution-Discretization Error: $\varepsilon = \|\mathbf{e}_J\|_\infty$ (without discontinuity)

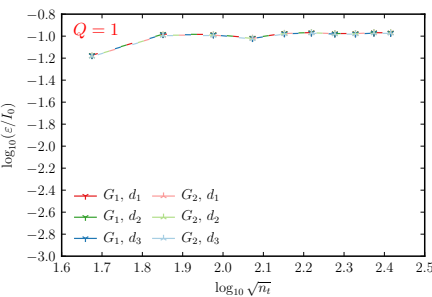
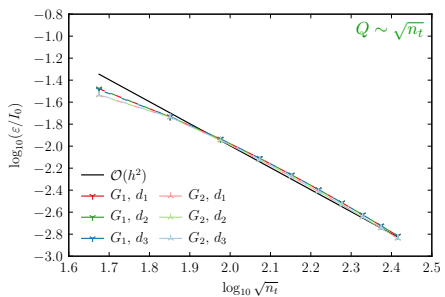


- Discontinuity removed from \mathbf{Z} using \mathbf{C} , corresponding MMS source term omitted in \mathbf{V}^ε :

$$\begin{bmatrix} \mathbf{A} & \mathbf{B} \\ \mathbf{C} & \mathbf{D} \end{bmatrix} \begin{Bmatrix} \mathbf{J}^h \\ \mathbf{I}^h \end{Bmatrix} = \begin{Bmatrix} \mathbf{V}^\varepsilon \\ \mathbf{0} \end{Bmatrix} \rightarrow \begin{bmatrix} \mathbf{A} & (\mathbf{B}_1 + \mathbf{B}_2) \\ \mathbf{C} & \mathbf{D} \end{bmatrix} \begin{Bmatrix} \mathbf{J}^h \\ \mathbf{I}^h \end{Bmatrix} = \begin{Bmatrix} \mathbf{V}^\varepsilon \\ \mathbf{0} \end{Bmatrix}$$

- Convergence rates for $Q = 1$ and $Q \sim \sqrt{n_t}$ are $\mathcal{O}(h^2)$
- Correct implementation of \mathbf{B}_1 suggested by its removal using \mathbf{C}
- Correct implementation of \mathbf{C} suggested by expected convergence rates

Solution-Discretization Error: $\varepsilon = \|\mathbf{e}_I\|_\infty$ (without discontinuity)



- Discontinuity removed from \mathbf{Z} using \mathbf{C} , corresponding MMS source term omitted in \mathbf{V}^ε :

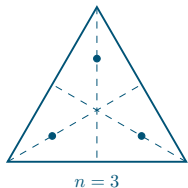
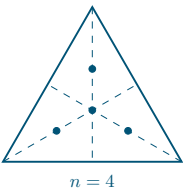
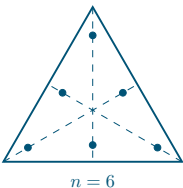
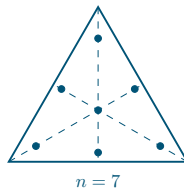
$$\begin{bmatrix} \mathbf{A} & \mathbf{B} \\ \mathbf{C} & \mathbf{D} \end{bmatrix} \begin{Bmatrix} \mathbf{J}^h \\ \mathbf{I}^h \end{Bmatrix} = \begin{Bmatrix} \mathbf{V}^\varepsilon \\ \mathbf{0} \end{Bmatrix} \rightarrow \begin{bmatrix} \mathbf{A} & (\mathbf{B}_1 + \mathbf{B}_2) \\ \mathbf{C} & \mathbf{D} \end{bmatrix} \begin{Bmatrix} \mathbf{J}^h \\ \mathbf{I}^h \end{Bmatrix} = \begin{Bmatrix} \mathbf{V}^\varepsilon \\ \mathbf{0} \end{Bmatrix}$$

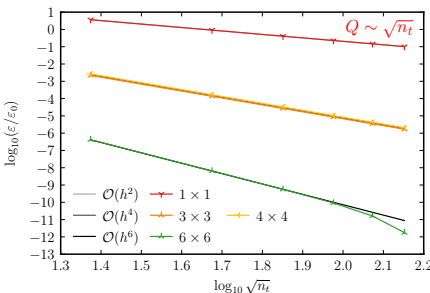
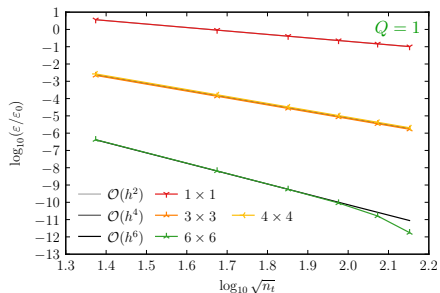
- Convergence rates for $Q = 1$ and $Q \sim \sqrt{n_t}$ are $\mathcal{O}(h^2)$ and $\mathcal{O}(1)$
- Correct implementation of \mathbf{B}_1 suggested by its removal using \mathbf{C}
- Correct implementation of \mathbf{C} suggested by expected convergence rates

Numerical Integration

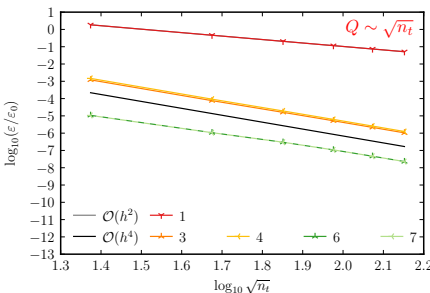
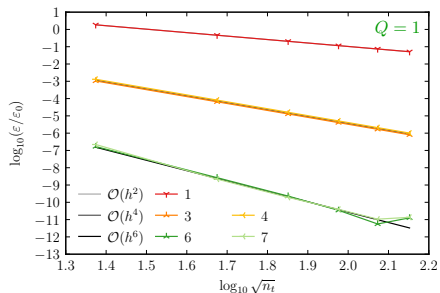
- Surface integrals evaluated using 2D triangle quadrature rules
- Wire integrals evaluated using 1D bar quadrature rules

Maximum integrand degree	Number of 2D points	Number of 1D points	Convergence rate
1	1	1	$\mathcal{O}(h^2)$
2	3	—	$\mathcal{O}(h^4)$
3	4	2	$\mathcal{O}(h^4)$
4	6	—	$\mathcal{O}(h^6)$
5	7	3	$\mathcal{O}(h^6)$

 $n = 3$  $n = 4$  $n = 6$  $n = 7$

Numerical-Integration Error: $\varepsilon = |e_a|$ ($G = G_2$, $d = d_1$)

- 2D points: [number for test integral] \times [number for source integral]
- 1D points: number of 1D points with same convergence rate as 2D points
- Convergence rates are as expected for $Q = 1$ and $Q \sim \sqrt{n_t}$

Numerical-Integration Error: $\varepsilon = |e_b|$ ($G = G_2$, $d = d_1$)

- 2D points: number for test integral
- 1D points: number of 1D points with same convergence rate as 2D points
- Convergence rates are as expected for $Q = 1$
- Convergence rates are limited to $\mathcal{O}(h^4)$ for $Q \sim \sqrt{n_t}$ since $\left| \int_0^L (I_{m_Q}(s) - I_m(s)) ds \right|$ is $\mathcal{O}(Q^{-4})$

Outline

- Introduction
- Governing Equations
- Code-Verification Approaches
- Numerical Examples
- Summary
 - Closing Remarks

Closing Remarks

3 error sources in electromagnetic integral equations:

- **Domain-discretization error** – avoided
 - Considered planar surfaces
- **Solution-discretization error** – isolated
 - Manufactured \mathbf{J} , chose \mathbf{I}_m to avoid source term
 - Manufactured Green's function (to integrate exactly)
 - Removed discontinuity to measure convergence rates without contamination
 - Demonstrated implications of sine series truncation error on convergence
- **Numerical-integration error** – isolated
 - Removed solution-discretization error
 - Demonstrated implications of sine series truncation error on convergence

Achieved expected orders of accuracy

Questions?

bafreno@sandia.govbrianfreno.github.io

Additional Information

- B. Freno, N. Matula, W. Johnson
Manufactured solutions for the method-of-moments implementation of the EFIE
Journal of Computational Physics (2021) [arXiv:2012.08681](https://arxiv.org/abs/2012.08681)
- B. Freno, N. Matula, J. Owen, W. Johnson
Code-verification techniques for the method-of-moments implementation of the EFIE
Journal of Computational Physics (2022) [arXiv:2106.13398](https://arxiv.org/abs/2106.13398)
- B. Freno, N. Matula
Code verification for practically singular equations
Journal of Computational Physics (2022) [arXiv:2204.01785](https://arxiv.org/abs/2204.01785)
- B. Freno, N. Matula
Code-verification techniques for the method-of-moments implementation of the MFIE
Journal of Computational Physics (2023) [arXiv:2209.09378](https://arxiv.org/abs/2209.09378)
- B. Freno, N. Matula
Code-verification techniques for the method-of-moments implementation of the CFIE
Journal of Computational Physics (2023) [arXiv:2302.06728](https://arxiv.org/abs/2302.06728)
- B. Freno, N. Matula, R. Pfeiffer, E. Dohme, J. Kotulski
Manufactured solutions for an electromagnetic slot model
Journal of Computational Physics (2024) [arXiv:2406.14573](https://arxiv.org/abs/2406.14573)
- B. Freno, N. Matula, R. Pfeiffer, V. Dang
Code-verification techniques for an arbitrary-depth electromagnetic slot model
Engineering Analysis with Boundary Elements (2025) [arXiv:2503.04004](https://arxiv.org/abs/2503.04004)

